Available online at www.CivileJournal.org

Civil Engineering Journal

(E-ISSN: 2476-3055; ISSN: 2676-6957)

Vol. 9, No. 09, September, 2023

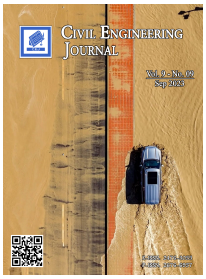

# An Intelligent Approach for Predicting Mechanical Properties of High-Volume Fly Ash (HVFA) Concrete

Musa Adamu [1*], A. Batur Çolak [2], Ibraim K. Umar [3], Yasser E. Ibrahim [1], Mukhtar F. Hamza [4]

[1] *Engineering Management Department, College of Engineering, Prince Sultan University, 11586 Riyadh, Saudi Arabia.*

[2] *Information Technologies Application and Research Center, Istanbul Ticaret University, Istanbul 34445, Türkiye.*

[3] *Department of Civil Engineering, Kano State Polytechnics, Kano, Nigeria.*

[4] *Department of Mechanical Engineering, College of Engineering, Prince Sattam Bin Abdulaziz University, Alkharj 16273, Saudi Arabia.*

Received 23 June 2023; Revised 18 August 2023; Accepted 24 August 2023; Published 01 September 2023

**Abstract**

Plastic waste (PW) is a major soild waste, which its generation continues to increase globally year in and year out. Proper management of the PW is still a challenge due to its non-biodegradable nature. One of the most convenient ways of managing plastic waste is by using it in concrete as a partial substitute for natural aggregate. However, the main shortcomings of adding plastic waste to concrete are a reduction in strength and durability. Hence, to reduce the undesirable impact of the PW in concrete, highly reactive additives are normally added. In this research, 240 experimental datasets were used to train an artificial neural network (ANN) model using Levenberg Marquadt algorithms for the prediction of the mechanical properties and durability of high-volume fly ash (HVFA) concrete containing fly ash and PW as partial substitutes for cement and coarse aggregate, respectively, and graphene nanoplatlets (GNP) as additives to cementitious materials. The optimized model structure has five input parameters, 17 hidden neurons, and one output layer for each of the physical parameters. The results were analyzed graphically and statistically. The obtained results revealed that the generated network model can forecast with deviations less than 0.48%. The efficiency of the ANN model in predicting concrete properties was compared with that of the SVR (support vector regression) and SWLR (stepwise regression) models. The ANN outperformed SVR and SWLR for all the models by up to 6% and 74% for SVR and SWLR, respectively, in the confirmation stage. The graphical analysis of the results further demonstrates the higher prediction ability of the ANN.

*Keywords:* Plastic Waste; Fly Ash; Graphene Nanoplatelets (GNP); ANN; SVM; SWLR.

## 1. Introduction

Plastic waste (PW) is one of the most generated and disposed of solid wastes globally due to the continuous usage of plastic materials in almost all areas of life, ranging from schools, hospitals, homes, markets, industries, etc. Due to its nonbiodegradable nature, proper disposal and management of the PW becomes a major challenge for most nations, especially developing and underdeveloped countries [1–3]. According to the United Nations Environment Programme UN Environment Programme [4] (UNEP 2022), globally, about 1 million plastic bottles are purchased per minute, while about five trillion plastic bags are utilized annually. Out of the plastic materials used, about 50% are used for a single

* Corresponding author: madamu@psu.edu.sa

http://dx.doi.org/10.28991/CEJ-2023-09-09-04

purpose and then disposed of in the environment. The estimated global PW generation has reached around 400 million metric tons per year, with this number projected to reach 1.1 billion metric tons by 2050. Out of this amount of PW generated, only about 15% is properly treated or reused, with about 85% of it discarded as unregulated waste or in landfills [4]. When PW is discarded in landfills, it causes several undesirable and harmful effects on the environment due to its nonbiodegradability and chemically non-reactive nature with the environment, as it will not decompose even after centuries. With time, the disposed PW will begin to release poisonous or toxic chemicals and gases into the environment, polluting the soil, air, and underground water. When disposed into the ocean, rivers, or seas, the toxic gases or chemicals leaching out of the PW can pollute the water and even affect the lives of aquatic animals. Using PW as a source of power through burning might be an alternative to its disposal; however, the negative effects of burning the PW include the release of $CO_2$, poisonous fly ash, and toxic chemicals [2, 5].

The utilization of PW as aggregate in buildings and construction is one of the most viable solutions to issues related to its disposal. This is because concrete, which is the most commonly used construction material, contains about 80% aggregate as its constituent material. Therefore, proper utilization of the PW in concrete will significantly reduce the amount disposed of in landfills and reduce the dependency on natural aggregates for making concrete, thus enhancing environmental and material sustainability. Furthermore, PW as an aggregate in concrete enhanced some properties of the concrete. However, PW was reported to have a negative influence on the mechanical properties and durability performance of concrete [6–8]. Nevertheless, there are several benefits to using PW as a substitute for aggregates in concrete. Some of the advantages of adding PW to concrete include enhancements in impact resistance, energy absorption, and ductility. Furthermore, due to its fibrous nature, PW prevents crack formation and limits its propagation in concrete structures before failure occurs. Furthermore, PW can enhance the flexural strength and toughness of reinforced concrete structures, especially in the tension zone [9, 10]. PWs are usually used in producing concrete barriers on roads to minimize accidents due to impacts or collisions with the barriers [8, 11]. Another benefit of using PW in concrete is that it increases the thermal insulation properties of concrete, mortar, and blocks due to its lower thermal conductivity in comparison to mineral aggregates. Thus, if used in buildings, PW is expected to reduce the needed energy for cooling the structure [12, 13].

For proper utilization and acceptance of PW as a partial or complete replacement for aggregates in concrete, there is a need to devise proper measures to reduce and limit its deleterious effects on the concrete's properties. Some researchers added highly reactive pozzolanic materials, either as a partial replacement or additive to cement, to the concrete containing PW. Farajzadehha et al. [14] reported that using nano silica as an additive in concrete containing PW enhanced its mechanical strengths. Adamu et al. [2] also reported that graphene nanoplatelets (GNP) as an additive to concrete containing PW as aggregates enhanced and partially mitigated the loss in mechanical strengths, while up to 0.225% GNP as an additive by cement weight totally mitigated the loss in strengths in concrete containing up to 15% PW as a partial substitute for coarse aggregates. Ahmad et al. [15] also found that the addition of GNP as an additive to PW concrete mitigated the loss in mechanical strength caused by the concrete. They found that 5% GNP addition by cement mass totally mitigated the loss of strength in concrete containing 25% PW as a partial substitute for coarse aggregate. For concrete containing 25% PW and 5% GNP, its compressive strength improved by 13.6% while its flexural strength enhanced by 31.4% compared to the plain concrete. Adamu et al. [3] reported that using silica fume to partially replace 10 to 20% of cement in concrete containing up to 20% PW as fine aggregate replacement significantly mitigated the loss in compressive and tensile strengths of the concrete due to the negative effect of PW. According to the findings of Punitha et al. [16], exchanging 10% cement with metakaolin partially mitigated the loss in strength in concrete containing up to 15% PW as a replacement for fine aggregate. According to the findings of Balasubramanian et al. [17], replacement of up to 15% cement with waste ground powder mitigated the reduction in strengths in concrete containing up to 15% PW as a substitute for coarse aggregates. A few studies adopted some methods of reducing the undesirable effect of PW on concrete's properties. Studies by Liu et al. [18] showed that subjecting the PW to Gamma radiations before adding it to concrete led to an enhancement in the mechanical strengths of the concrete, where the negative effect of replacing up to 7% fine aggregate with PW on the strengths of the concrete was totally mitigated. Khan et al. [19] also reported that exposing PW to gamma rays before adding it to grout significantly diminishes the loss in strength caused by the negative effect of the PW.

The artificial intelligence approach is established as complementary to conventional mathematical tools and is widely used in many areas for predicting the performance of structures or systems using existing data. ANN is one of the artificial intelligence tools that have high accuracy of prediction ability with their powerful structures and learning capabilities. ANN has been applied in the areas of building and construction for the prediction of concrete's properties. Çolak et al. [20] applied ANN to examine the influence of elevated temperature on the properties of mortar containing PW as a partial replacement for fine aggregates. They subjected the mortar to temperature exposures between 100 and 400 °C for up to 3 hours. They utilized ANN to develop models for predicting the compressive and bending strengths of the mortar. Their results disclosed that increasing temperature and the amount of PW in the mortar caused a decline in compressive and flexural strengths. The established ANN models were able to predict the strengths of the mortar with a mean error of -0.51%. Çelik et al. [21] established ANN models for predicting the Marsh cone flow time, mini-slump

propagation diameter, and plate cohesion of a grouting material. The proposed ANN model was able to predict mini collapse propagation diameter, Marsh cone flow time, and plate cohesion value with very low error rates. Çolak, et al. [22] used an MLP-ANN model for the prediction of the workability of mortar produced with fly ash and nanosilica as binder materials. In the study on predictive values, it has been seen that the MLP network can predict the workability properties with ideal precision. Rezvan et al. [23] employed the ANN technique to investigate the advantages of using polyethylene terephthalate (PET) PW as a fiber material in concrete. Their proposed ANN model can predict the mechanical properties of the PET fiber-reinforced concrete with a 98% coefficient of correlation and a 7.11 MPa mean square error (MSE). Sau et al. [24] adopted ANN for the prediction of the fresh and hardened properties of concrete containing PW as a partial substitute for fine aggregate, where they used replacement levels between 5 to 40%. They found that the ANN technique has excellent prediction ability; it was able to predict the fresh and hardened properties of the concrete with up to a 99% degree of determination.

Ofuyatan et al. [25] used ANN and response surface methodology (RSM) to predict the mechanical properties of self-compacting concrete (SCC) containing silica fume and PW as partial substitutes for cement and fine aggregates, respectively. They replaced between 0 to 20% of the fine aggregate with PW and 0 to 40% of the cement with silica fume. From their findings, both ANN and RSM models can accurately predict the compressive strengths and other hardened properties of the SCC. The ANN model has the best predicting power, where it has an $R^2$ value of 0.93 for the compressive strength model at the stages of training, testing, and validation. Furthermore, the ANN model has higher suitability for the datasets. Nafees et al. [26] utilized different machine learning techniques (individual and ensemble) for creating models for the prediction of compressive and tensile strengths. They used PW to partially replace either fine aggregate or cement in the concrete and cast 160 cylinders, testing them for compressive and split tensile strengths in the laboratory. Furthermore, for the models, they used an addition of about 320 datasets each for the compressive and split tensile strengths from existing literature. They used multilayer perceptron neural networks (MLPNN), support vector machines (SVM), and other machine learning techniques. From their findings, the ensemble models with boosting and bagging have better performance with fewer errors compared to the individual models. The models have high performance, with coefficients of correlation up to 0.932 and 0.86 for the compressive and split tensile strengths, respectively. They concluded that the machine learning techniques were used to predict the mechanical properties of the PW concrete to promote sustainability.

Given the advantages and shortcomings of using PW as aggregates in concrete and the methods devised to completely or partially mitigate the loss in mechanical strength of concrete due to the undesirable effects of PW. Producing concrete using PW with improved or acceptable strengths for structural applications will significantly reduce the dependency on natural aggregates for making concrete, which will reduce the depletion of natural resources. Furthermore, this improves environmental sustainability through proper PW disposal. However, most of the methods developed for reducing the negative effects of PW on the mechanical properties of concrete are not cost-effective and sometimes do not significantly mitigate the loss in strength. Hence, this led to the use of graphene nanomaterials due to their high reactivity and fine sizes. Studies by Adamu et al. [2] have shown that when graphene nanoplatelets (GNP) were used as additives in concrete containing PW, it significantly mitigated the loss in mechanical strengths due to the negative effect of the PW.

ANN is now one of the most acceptable and precise methods of predicting the behavior or properties of materials. Many studies have utilized ANN techniques to predict the properties of concrete containing PW. However, the use of GNP to reduce the negative effects of PW in concrete is still in its early stages, and there are few studies that have employed GNP as an additive in PW concrete. Furthermore, ANN techniques have been able to predict the properties of concrete. There is a need to employ ANN techniques to predict the mechanical properties of concrete containing PW with GNP added to mitigate the negative effect of the PW. To the best knowledge of the authors, there are no available studies that utilized ANN techniques for the modeling and prediction of the mechanical properties of PW concrete modified with GNP as an additive to cement to mitigate the negative effects of the PW. Therefore, in this study, the ANN technique was used to predict the mechanical strengths of HVFA-modified PW as a partial substitute for coarse aggregates and GNP as an additive to cementitious materials.

## 2. Data and Analysis Method

The study was conducted in two stages. In the first stage, a multilayer perceptron feed-forward neural network (MLP-FFNN) was used for predicting the mechanical properties of concrete modified with plastic waste, fly ash, and graphene nanoplatelets. Finally, the results of the MLP-FFNN models were compared with those of the support vector regression (SVR) model and stepwise regression (SWLR) model. The schematic of the proposed methodology is given in Figure 1.

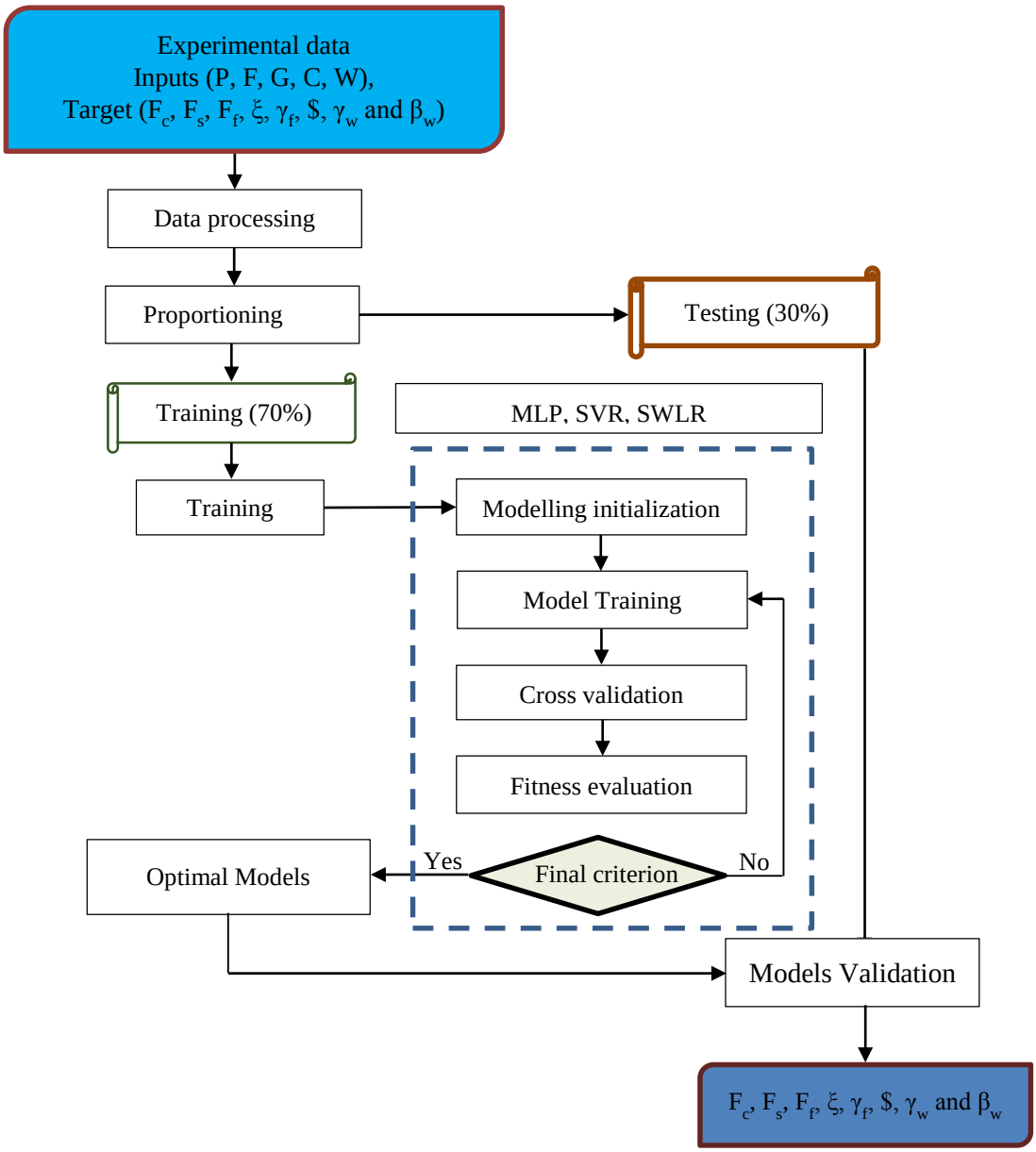


**Figure 1. Proposed Schematic of Methodology**

***Data***

For a supervised machine learning algorithms, several input variables are needed to give the predicted response in form of outputs. The experimental data used for devloping the prediction models for the mechanical properties of the concrete using fly ash, PW and GNP as the input variables was obtained from previous study by Adamu et al. [2], where a total of 240 data sets (mixes) were used for training, testing and validation. Five input variables were used as summarized in Table 1. The number of output variables i.e. predicted responses are eight as depicted in Table 1.

**Table 1. Input and Output Variables used for ANN Modelling**

| **Input Variables** | | | **Predicted Responses (Output Variables)** | | |
|---|---|---|---|---|---|
| **Variables** | **Symbol** | **Units** | **Outputs** | **Symbols** | **Units** |
| Plastic Waste | P | % | Slump | $ | mm |
| Fly Ash | F | % | Fresh Density | $\gamma_f$ | kg/m$^3$ |
| Graphene Nanoplatelets (GNP) | G | % | Unit Weight | $\gamma_w$ | kg/m$^3$ |
| Curing Periods | C | Days | Compressive Strength | $F_c$ | MPa |
| Water-to-binder | W | - | Split tensile strength | $F_s$ | MPa |
| | | | Flexural strength | $F_f$ | MPa |
| | | | Elastic Modulus | ξ | GPa |
| | | | Water Absorption | $\beta_w$ | % |

## 2.1. ANN Modelling

Models have been established to analyze and predict the mechanical properties of concrete containing fly ash, PW, and GNP using the ANN approach. The established ANN models were designed in multi-layer perceptron (MLP) architecture as an extensively used structure with its strong structure. MLP networks are structurally composed of layers, and each layer is directly linked to the others. First is the input layer, where all the independent variables are defined and described. Next is the hidden layer; all MLP networks consist of a minimum of one layer. The final layer is the output layer, where all the predicted properties were obtained. In the input layer of the developed ANN model, P, F, G, C, and W values were defined as input variables, and a total of eight responses, $F_c$, $F_s$, $F_f$, $\xi$, $\gamma_f$, \$, $\gamma_w$, and $\beta_w$, were estimated in the output layer. The basic design of the established MLP network is given in Figure 2. No fixed model is available for the determination of the number of neurons, which is a critical computational element in the MLP's hidden layer. This is one of the main shortcomings in creating MLP networks. To overcome this challenge, the number of neurons in the hidden layer was optimized by performing performance analyses of MLP networks with different neuron numbers. Figure 3 summarizes the essential MLP networks' structure, which contains 5 independent variables (input) in the input layer, 17 neurons in the hidden layer, and 8 output parameters in the output layer.

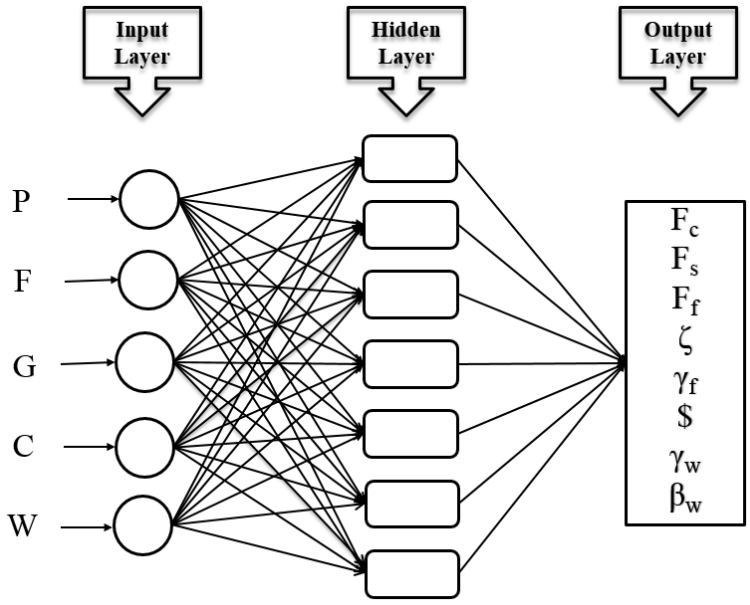


**Figure 2. The basic architecture of the developed MLP network**

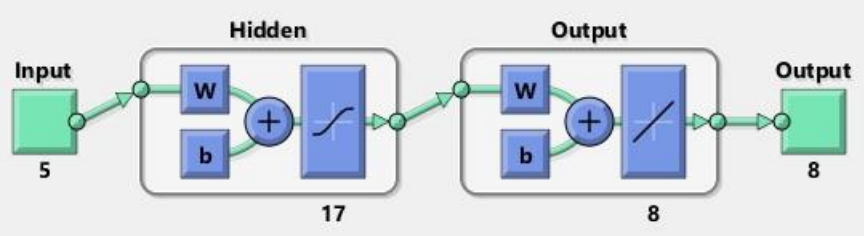


**Figure 3. The basic structure of the MLP network model**

In the establishment of the ANN models, it is vital to carry out optimization of the data set in an ideal way. For the ANN modeling, which was established using a set of 240 data points, the methodology available in existing studies was adopted for grouping the data [27, 28]. For the training phase of the model, 168 data sets were used, while for the testing and validation stages, 36 data sets were each used. The training algorithm of the model is the Levenberg-Marquard algorithm, which is one of the most commonly used algorithms in MLP networks. Tan-Sig and Purelin transfer functions were employed in the hidden and output layers of the MLP network, respectively. The mathematical expressions of the transfer functions used are given below [27, 28]:

$$f(x) = \frac{1}{1+\exp(-x)} \quad (1)$$

$$purelin(x) = x \quad (2)$$

One of the important steps in the establishment of ANN models is analyzing their performance in terms of prediction accuracy. For this purpose, mean squared error (MSE), coefficient of performance (R), and margin of deviation (MoD) parameters, which are widely used in the literature, were determined. The numerical expressions applied for calculating the model's performance parameters are expressed below [29, 30]:

$$MSE = \frac{1}{N}\sum_{i=1}^{N}(X_{exp(i)} - X_{ANN(i)})^2 \quad (3)$$

$$R = \sqrt{1 - \frac{\sum_{i=1}^{N}(X_{exp(i)} - X_{ANN(i)})^2}{\sum_{i=1}^{N}(X_{exp(i)})^2}} \quad (4)$$

$$MoD\ (\%) = \left[\frac{X_{exp} - X_{ANN}}{X_{exp}}\right] x\ 100 \quad (5)$$

### 2.2. Support Vector Regression (SVR) and Stepwise Linear Regression (SWLR)

Support vector regression (SVR) is a regression technique that is nonlinear in nature and is used to model complex nonlinear problems and processes. It is established based on the theory of support vector machines (SVM). Some of the advantages of SVR in modeling complex engineering problems include better noise tolerance, higher learning speed and accuracy, and exclusive generalization ability [31–33]. The main objective of SVR is to minimize operational risk, which is similar to other SVM techniques. The SVR differs from the black box technique, whose main aim is to minimize the errors between the predicted and measured values. For the SVR, two phases are involved: the first phase is to fit the data into a linear regression, and the second phase is to pass the output over a nonlinear kernel, which then returns the nonlinear shape of the data. SVR employs a kernel function to map the data to a higher-dimensional feature space from the sample space [32, 34].

On the other hand, stepwise regression (SWLR) is a linear regression technique best used for the description of the reliance between the input and output variables. Consequently, when expressing the reliance amongst the output variables and many free variables, it is crucial to obtain the best variable groups that create more precise prediction results in terms of the input variable [35]. SWLR is simply defined as a frontward selection process in which the set of optimum input variables is chosen through the removal or addition of the variable(s) that have the highest impact on the remaining sum of squares (SoS). A systematic refinement of the variables is normally done by the SWLR and is then done by reassessing the quality of the passed-added variables based on their partial SoS. However, when the partial SoS for any of the previously appended variables is not satisfied with a base rule for fitting the models, then the set of variables is shifted to an omission state in a stepwise approach pending each of the residual variables fulfilling the base rule [35].

## 3. Results and Discussions

### 3.1. ANN Model

The initial stage in examining the performance of the established ANN models in terms of predictability is to assess the correctness of the predicted outputs estimated from the ANN models with the experimental data. In this context, firstly, the compatibility of the values obtained from the ANN model with the target values was examined. The fact that the values obtained from the ANN model are in ideal agreement with the target values is considered a confirmation that the prediction performance of the model is high. Figure 4 presents the ANN outputs and targeted values for each of the data points used to develop the model. After examining the data points for all the outputs (8 responses), the predicted values from the ANN models were in very good harmony with the target values representing the experimental data. This perfect fitness of estimation and target values displays that the obtained ANN model can ideally predict eight different output parameters. After examining the fitness of the ANN outputs with the data set, the estimation error of the ANN model was examined comprehensively. Even though all the mechanical properties and durability parameters of the concrete were predicted with high accuracy, A nearly perfect goodness of fit was observed in Figures 4-a to 4d, which indicates higher accuracy of the ANN models in prediction of $F_c$, $F_s$, $F_f$, and $\xi$, which are the major indicators of concrete strength.

The parameters with relatively lower accuracy in comparison with $F_c$ and $F_f$ are $\gamma_f$ and \$. Several studies have also reported the suitability of a machine learning approach for the prediction of concrete strength with high accuracy and stability [36, 37]. MoD values express the deviation rates between the predicted values obtained from the ANN model and the target values. The low MoD values indicate that the model's estimation error is low. The MoD values for all the data points in the establishment of the ANN model network are depicted in Figure 5. When the MoD values acquired from the calculations for each of the 8 different output parameters were assessed, it was observed that they were on a line near the zero-deviation line in general. When MoD values are taken into consideration, they are found to be mostly very low. However, it should be understood that the average MoD values are also quite low. The low MoD values indicate that the outputs acquired from the ANN model have a very low margin of error with the experimental data.

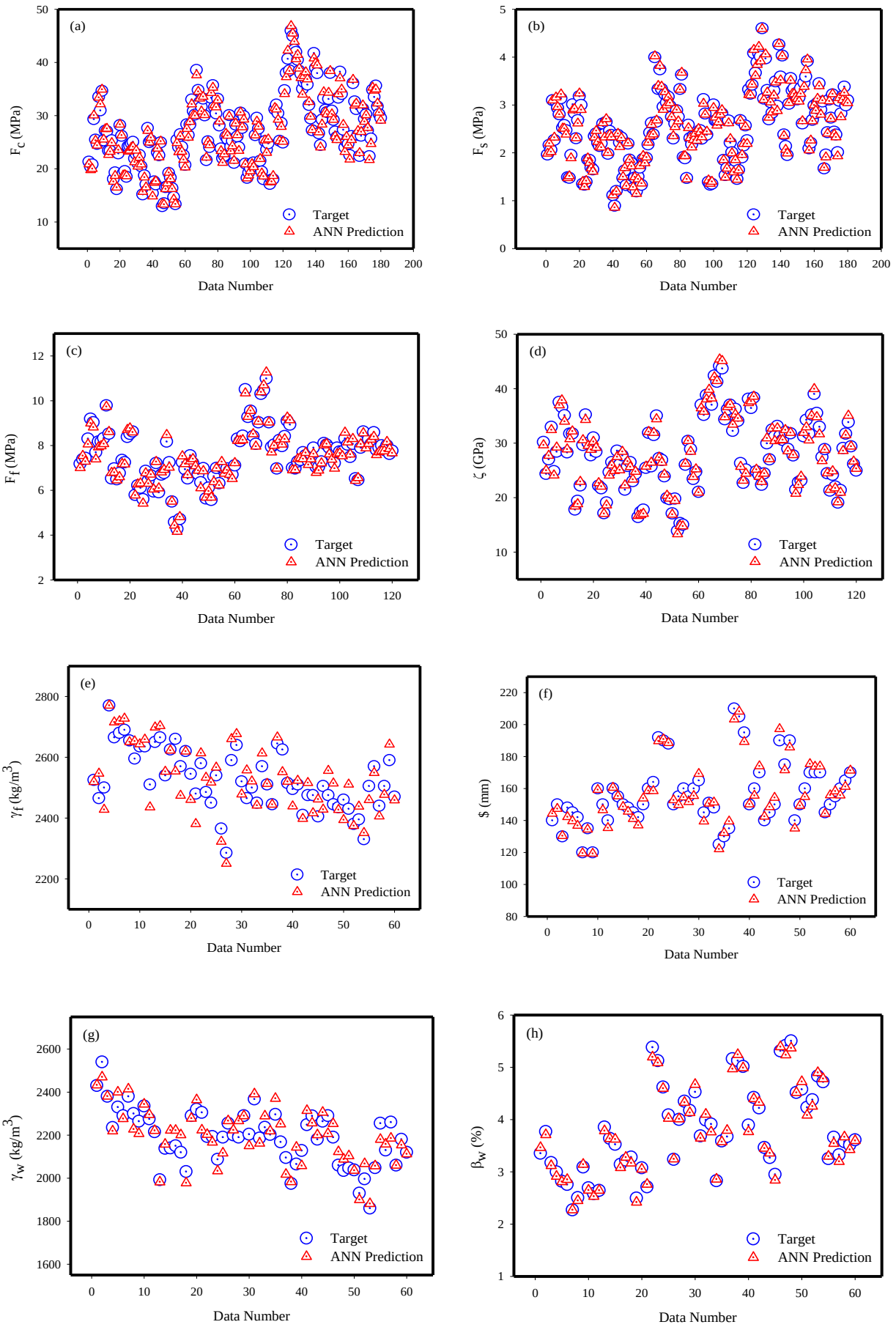


**Figure 4. The ANN outputs and target values for each of the data**

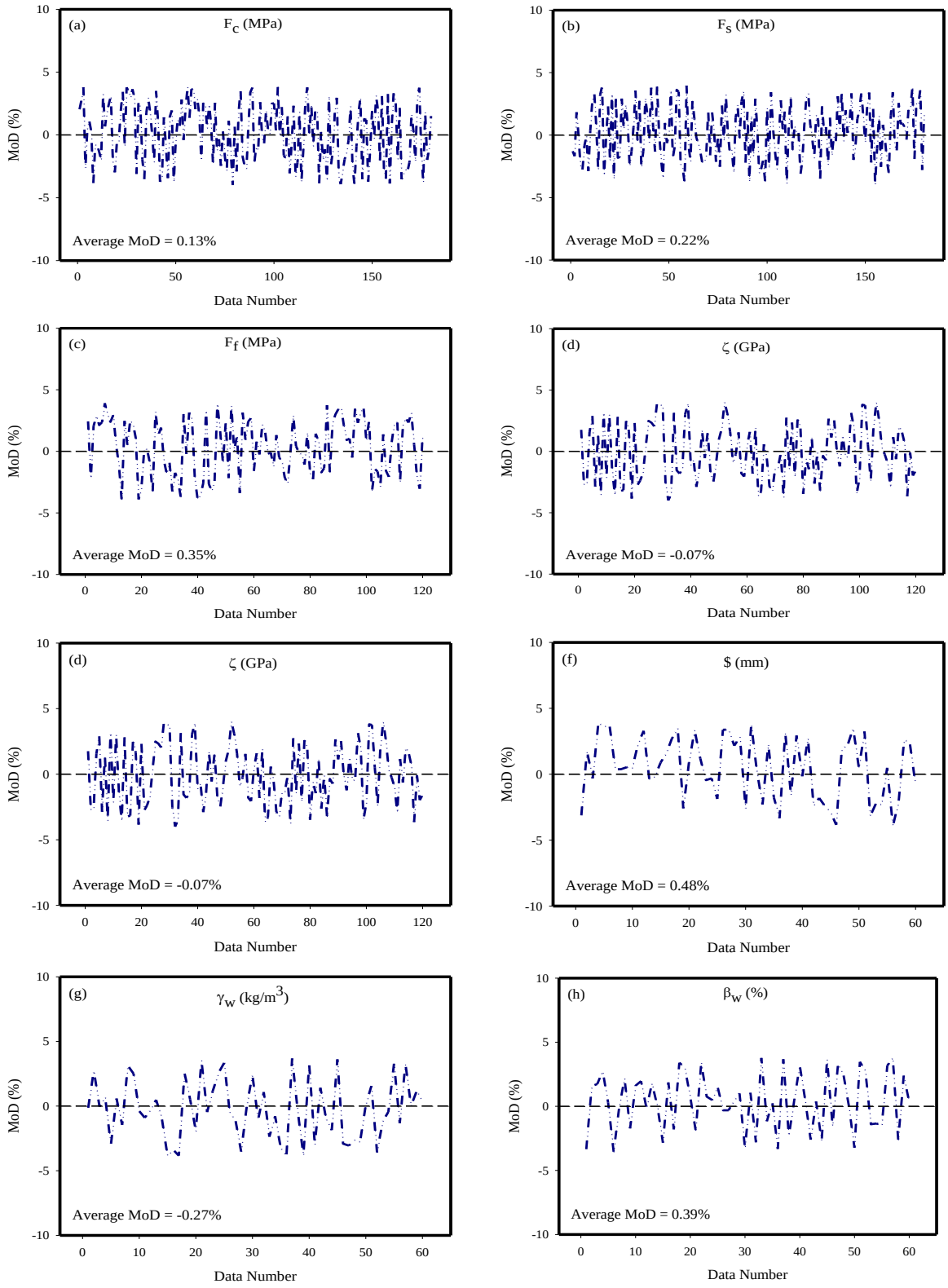


**Figure 5. The MoD values calculated for each data point**

Examination of MoD values gives sufficient information about the error rates of the ANN model. However, in order to make the prediction error analysis of the ANN model more comprehensive, it is important to examine the target values for each data point and the prediction values obtained from the ANN model. The low difference values indicate that the ANN model can predict with high accuracy for each data point. To further evaluate the models's goodness of fit, a scatter plot (Figure 6) presents the variations between the data sets and ANN model outputs calculated. This plot was used to make the analysis of the model's errors more comprehensive. After the discrepancy values presented for the eight different output values were assessed, it was found that a very low difference in terms of values was realized for each output value. All eight models have shown a high goodness of fit between the predicted and experimental data. It can clearly be seen that the data was compacted along the diagonal of the bisector (Figure 7). A perfect model will have

all the data along the diagonal bisector. The closer the data is to the diagonal bisector, the higher the accuracy. The results obtained from MoD and difference analyses revealed that the generated ANN model can estimate all eight output parameters with very low errors. In order to see the prediction accuracy of the ANN model more clearly, it was planned to perform the accuracy analysis of the model by creating a more comprehensive graph. Experimental data are placed on the x-axis of Figure 6, and the output values acquired from the ANN model are placed on the y-axis. Looking at the data points obtained for the 8 output values, it was generally observed that each of the data points was aligned very close to the zero-error line. However, it should be noticed that the data points also hang within the ±10% error band. For the developed ANN model, the MSE value was computed as 2.71E-03 and the R value as 0.99957. The nearness of the MSE and R values to zero and 1, respectively, is another piece of evidence that the established ANN model is proposed to carry out predictions with high accuracy.

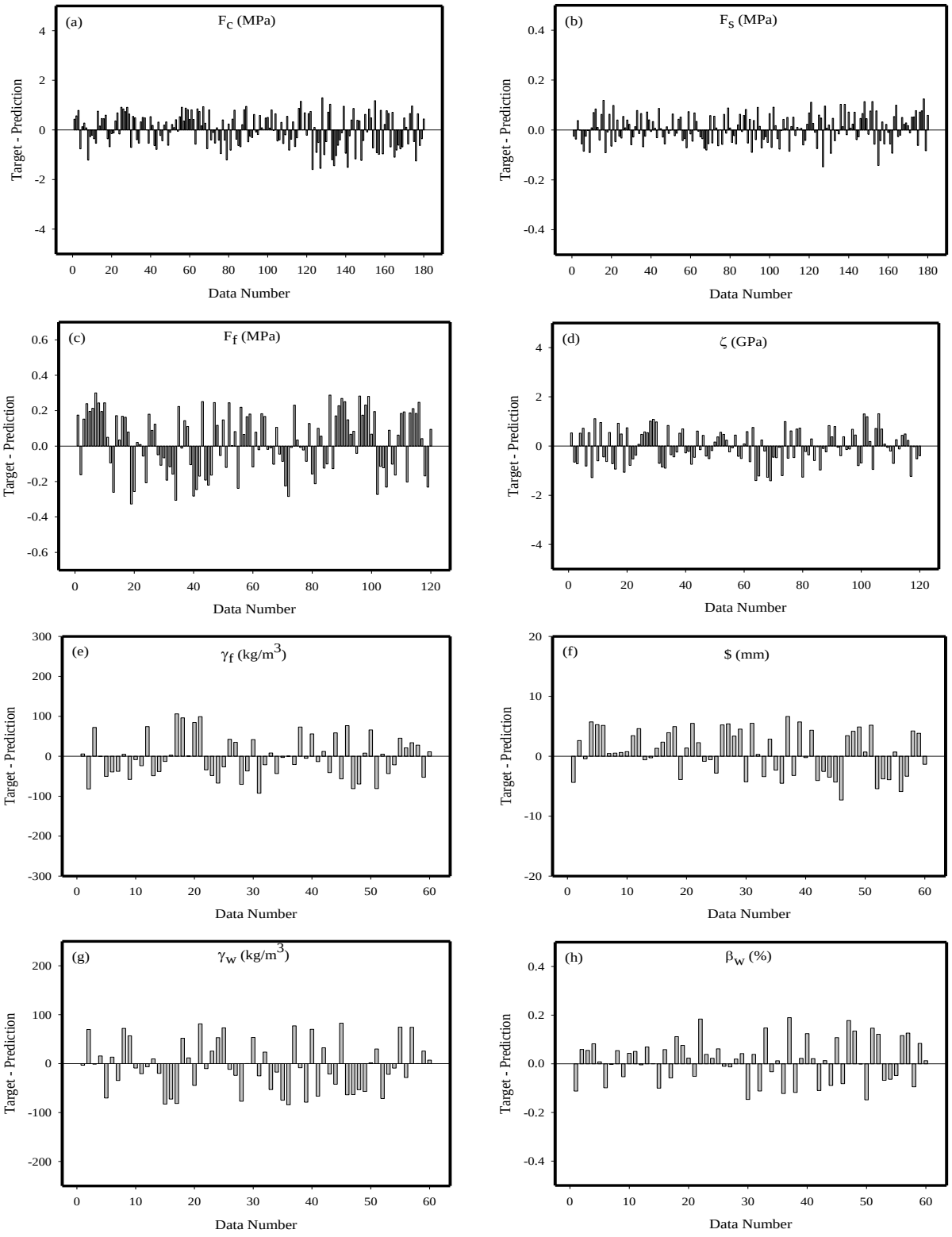


**Figure 6. The differences between the experimental data and the ANN outputs**

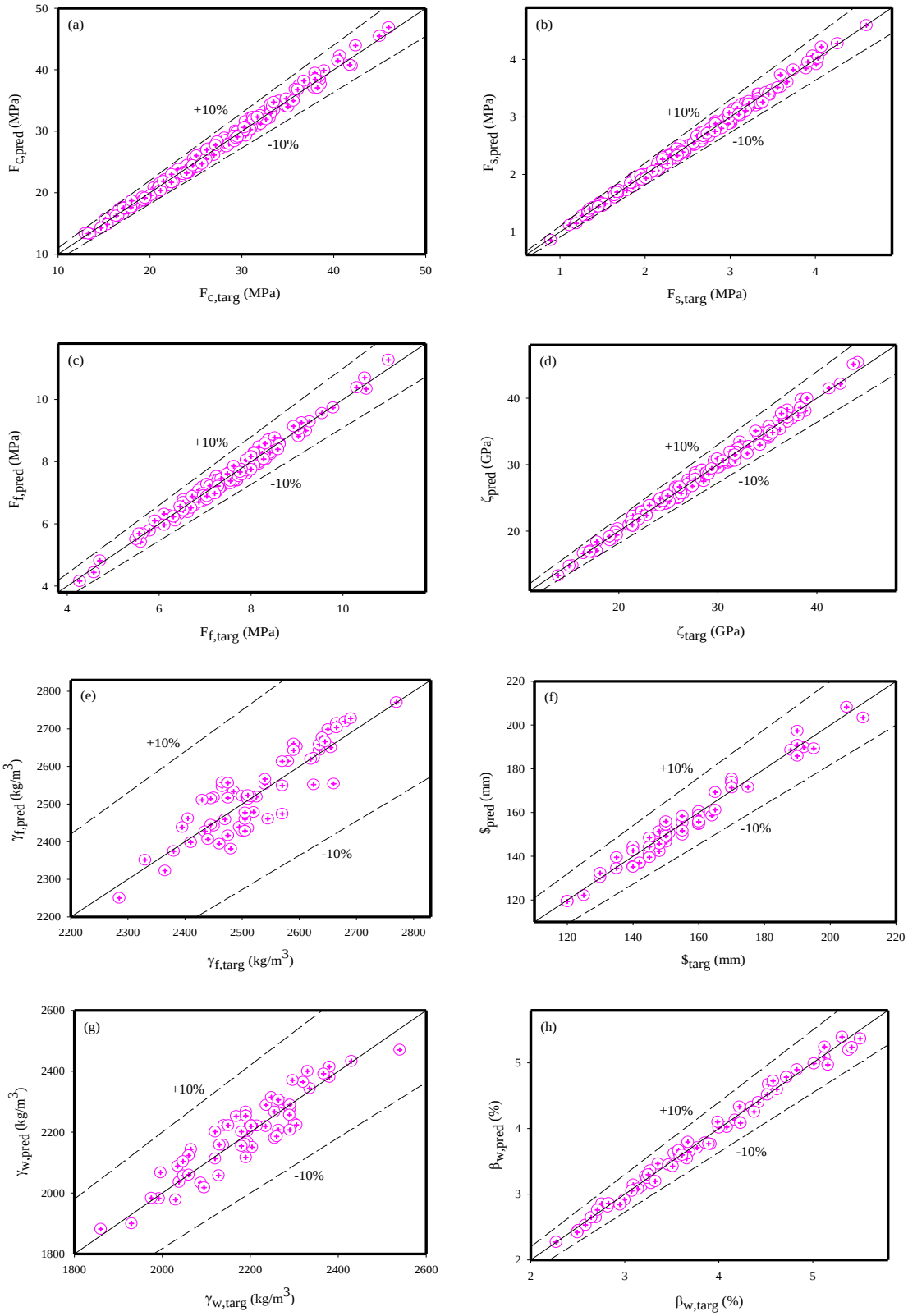


**Figure 7. Experimental and ANN predictions**

## 3.2. Support Vector Regression (SVR) and Stepwise Linear Regression (SWLR) Models

For comparison, SVR and SWLR were also used for the prediction of concrete properties. The modeling results indicated the superiority of the ANN models over both the SVR (nonlinear model) and SWLR, which is a nonlinear model, in terms of the prediction error. This is because the neuron in the ANN captures the data pattern more than the other models. The study results were further analyzed using two powerful graphical charts (the Taylor diagram and violin plots). The Taylor Plot (Figure 8) graphically compares three statistical measures of the models (correlation coefficient, standard deviation, and RMSE). Thus, it gives a separate and unswerving comparative assessment of the

three models in terms of performance accuracy and efficacy. The position of the azimuthal test field demonstrates the association between the estimated and observed results. The standard deviation (SD) for the experimental data set has a direct proportionality to the radiated value determined from the source. Additionally, the RMSE-centered value has a direct proportionality with the distance between the projected and experimental data, with a similar unit as the SD [38]. A faultless or good model is the one separated by the reference point with an equivalent CC value of 1, which looks alike with the profusion of diversities but is in contrast with the observations [39]. Additionally, the outcomes of the Taylor diagrams show that the ANN outshined the other two models (SVR and SWLR) with regards to all three statistical measures for all the concrete parameters. The CC values for all eight predicted concrete parameters (that is, fresh density, slump, unit weight, water absorption, compressive strength, flexural strength, and split tensile strength) are all greater than 0.99 for ANN and range from 0.99–0.95 for SVR. For the SWLR models, the CC values differ significantly. For example, the CC values for the unit weight and absorption models are between 0.99 and 0.95 while the CC values for compressive strength, flexural strength, split tensile strength, and elastic modulus range between 0.7-0.8 while those of fresh density and slump are between 0.5 and 0.6. This indicates the higher goodness of fit and estimation accuracy of the ANN models, followed by the SVR models, and lastly SWLR, as hinted by Zhu and Heddam [40]. This is because of the ability of the nonlinear models (ANN and SVR) to capture nonlinear patterns in the data. Also, in terms of error (RMSE), the ANN has the least error for all the models, followed by SVR and lastly SWLR. The models' SD was observed to be less than the experimental data, hence eliminating the overestimation problem. The ANN models replicate the experimental data more accurately than the SVR model and the linear SWLR model, and hence could be adopted by relevant stakeholders in concrete property modeling.

Finally, violin plots (Figure 9) were used to compare the models' performance further. Violin plots are used because of their advantage in combining distribution and box plots in addition to the interquartile ranges, median, and spread of observed data [32]. From Figure 8, it can be clearly observed that the shape of both the violin and box plot within it for the established ANN model looks more similar to the actual data compared to the SVR and SWLR models. This finding reveals that ANN can well mimic the data distribution, interquartile ranges, median, and data range for the eight concrete parameters. The overall assessment of the models using statistical and graphical measures (scatter plots, Taylor diagrams, and violin plots) proved increased prediction accuracy and error reduction in predicting the concrete parameters with the ANN models compared to SVR and SWLR.

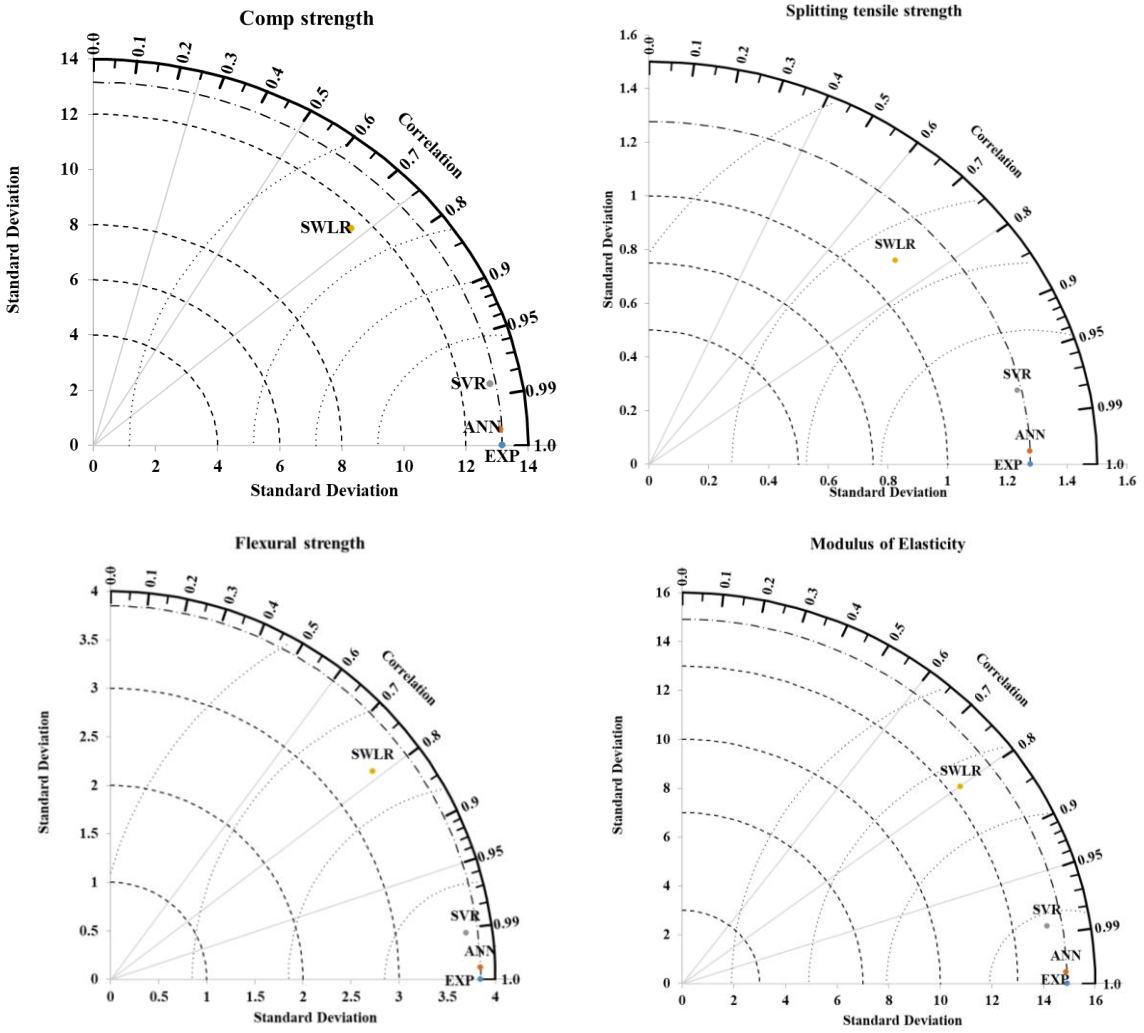

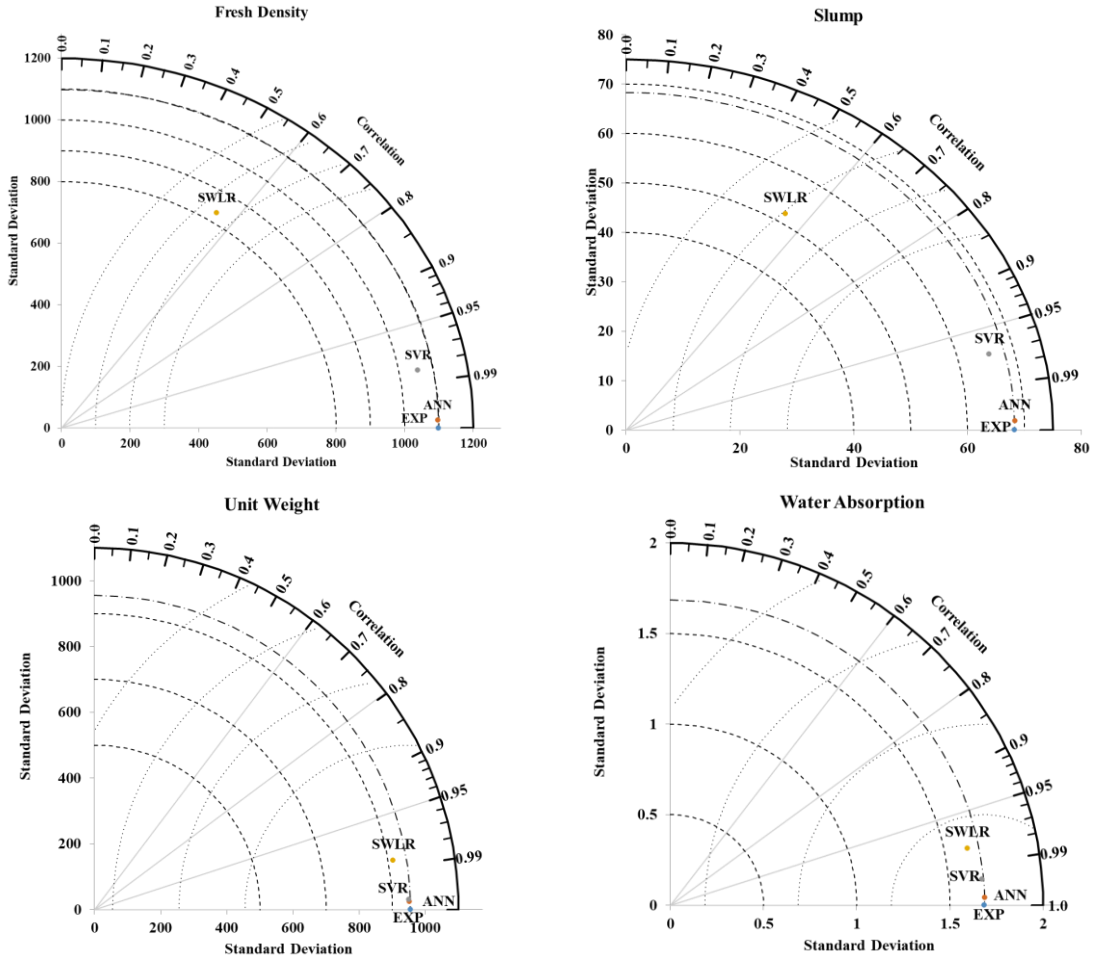


**Figure 8. Taylor plots comparing the performance of ANN, SVR, SWLR for the Eight Concrete parameters**

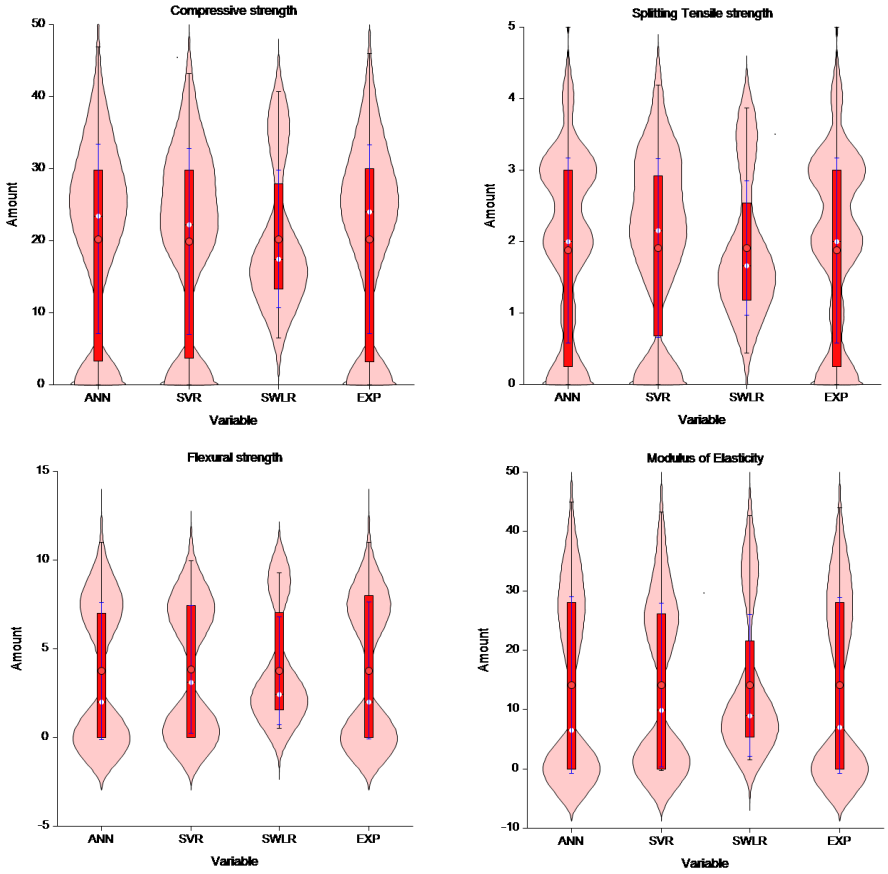

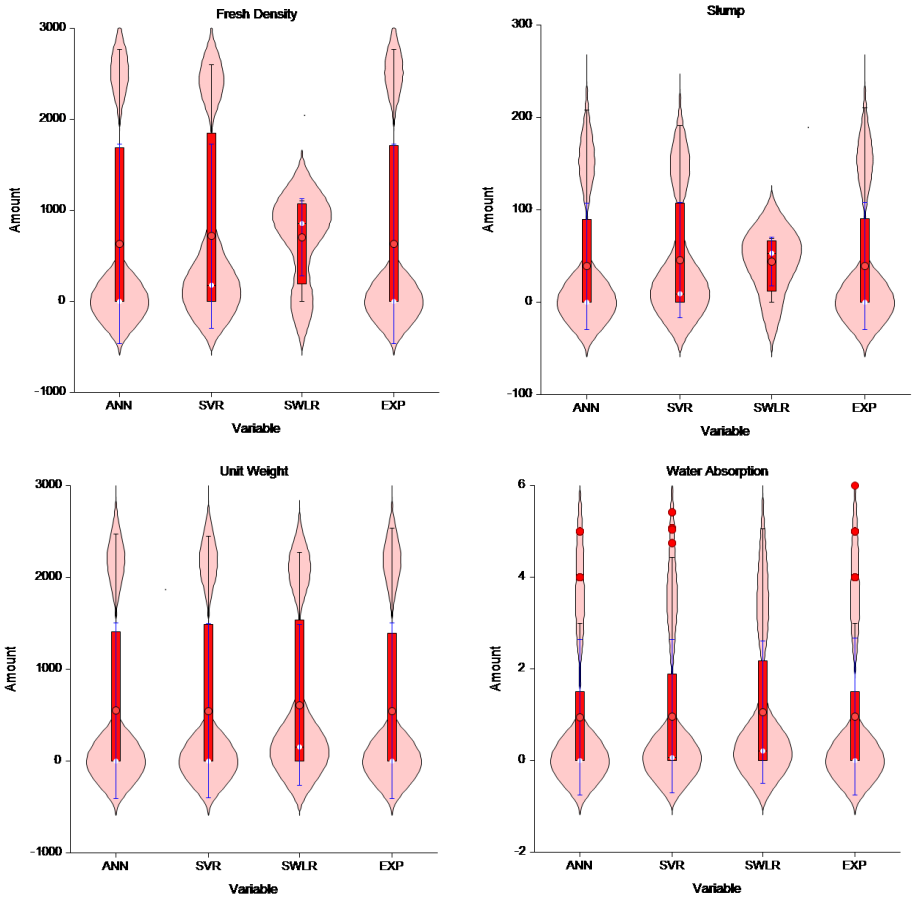


**Figure 9. Violin plots comparing the performance of ANN, SVR, SWLR for the 8 Concrete Properties**

Finally, the results of the present study were validated with literature. The validation was done based on the goodness of fit measures only as error measures might vary from one case study to another as per the data range. Musa et al. (2023) predicted the accuracy of concrete's flexural strength, compressive strength, and split tensile strength with an accuracy value of 0.9949. Haruna et al. [41] predicted the compressive strength of concrete modified with rice husk ash and calcium carbide waste using an emotional neural network and ANN with an $R^2$ value of 0.8951. Adamu et al. [37] predicted the compressive strength of concrete containing jujube seed as a partial replacement for coarse aggregate using the Hammerstein-Weiner (HW) and SVR models. The model predicted compressive strength with R values of 0.9953 and 0.9982 for HW and SVR, respectively. Based on the revealed prediction accuracy and in comparison, with the current research model accuracy, the ANN was able to obtain better predictability performance (R = 0.9994). Therefore, the application of ANN models to the prediction of the mechanical properties of concrete with high levels of accuracy and stability has been suggested.

## 4. Conclusion

In this study, ANN, SVR, and SWLR were used to develop models for forecasting and estimating the mechanical properties of HVFA concrete containing PW and GNP. An experimental dataset containing 240 datasets of P, F, G, C, W, $F_c$, $F_s$, $F_f$, ξ, $\gamma_f$, $, $\gamma_w$, and $\beta_w$ was used for conducting the study. The five input parameters P, F, G, C, and W were used to model each of the eight physical properties of the concrete. An ANN model trained using the Levenberg-Marquard algorithm predicted all eight concrete properties with a very good correlation and agreement between the estimated values from the ANN model and the experimental data. The MSE and R values of 2.71E-03 and 0.99957, respectively, explained the high accuracy of the prediction of the ANN model. From the deviation analysis, a 0.48% deviation value was found to be the highest deviation between the experimental and computed data using ANN. For comparison, SVR and SWLR were also employed for the prediction of the concrete properties. In addition to statistical analysis, two graphical charts (the Taylor diagram and Violin plots) were also used for comparing the accuracy and stability of the three models (ANN, SVR, and SWLR). The ANN outperformed both SVM and SWLR models by improving the performance efficiency of the models by up to 6% and 74%, respectively, for SVM and SWLR in the verification stage. These results have shown that the developed ANN model can forecast $F_c$, $F_s$, $F_f$, ξ, $\gamma_f$, $, $\gamma_w$, and $\beta_w$ values with very high accuracy. The major drawback of the study is that it did not show the degree to which each of the input parameters was affecting the properties of the concrete.

# 5. Declarations

## 5.1. Author Contributions

Conceptualization, M.A. and Y.E.I.; methodology, M.A.; software, A.B.Ç. and I.K.U.; validation, M.A., A.B.Ç., and M.F.H.; formal analysis, M.A., A.B.Ç., and I.K.U.; investigation, M.A. and Y.E.I.; resources, Y.E.I. and M.F.H.; data curation, M.A. and M.F.H.; writing—original draft preparation, M.A., A.B.Ç., and I.K.U.; writing—review and editing, Y.E.I. and M.F.H.; visualization, M.A. and Y.E.I.; supervision, Y.E.I.; funding acquisition, M.A. and Y.E.I. All authors have read and agreed to the published version of the manuscript.

## 5.2. Data Availability Statement

The data presented in this study are available on request from the corresponding author.

## 5.3. Funding

The authors also wish to acknowledge Prince Sultan University, Riyadh Saudi Arabia for covering the article processing charges.

## 5.4. Acknowledgements

The authors wish to acknowledge the support of the Structures and Materials Laboratory of the College of Engineering, Prince Sultan University, Riyadh, Saudi Arabia. The authors also wish to acknowledge the Center of Excellence in Innovative Construction Materials, Department of Civil Engineering, Chulalongkorn University, and the C2F scholarship at Chulalongkorn University in Bangkok, Thailand, for their viable support. Additionally, the author (Mukhtar F. Hamza) would like to thank Prince Sattam bin Abdulaziz University for supporting this work under project number PSAU/2023/R/1444.

## 5.5. Conflicts of Interest

The authors declare no conflict of interest.

# 6. References

[1] Mrowiec, B. (2018). Plastics in the circular economy (CE). Environmental Protection and Natural Resources, 29(4), 16–19. doi:10.2478/oszn-2018-0017.

[2] Adamu, M., Trabanpruek, P., Jongvivatsakul, P., Likitlersuang, S., & Iwanami, M. (2021). Mechanical performance and optimization of high-volume fly ash concrete containing plastic wastes and graphene nanoplatelets using response surface methodology. Construction and Building Materials, 308, 125085. doi:10.1016/j.conbuildmat.2021.125085.

[3] Adamu, M., Trabanpruek, P., Limwibul, V., Jongvivatsakul, P., Iwanami, M., & Likitlersuang, S. (2022). Compressive Behavior and Durability Performance of High-Volume Fly-Ash Concrete with Plastic Waste and Graphene Nanoplatelets by Using Response-Surface Methodology. Journal of Materials in Civil Engineering, 34(9), 4022222. doi:10.1061/(asce)mt.1943-5533.0004377.

[4] United Nation Environment Programme. (2022). Our planet is choking on plastic - Beat Plastic Pollution. United Nations, New York, United States. Available online: https://www.unep.org/interactives/beat-plastic-pollution/ (accessed on July 2023).

[5] Denta, S. M. (2022). End Plastic Pollution and Plastic Waste-Regulations and Collaboration. Copenhagen Business School, CBS LAW Research Paper.

[6] Bahij, S., Omary, S., Feugeas, F., & Faqiri, A. (2020). Fresh and hardened properties of concrete containing different forms of plastic waste – A review. Waste Management, 113, 157–175. doi:10.1016/j.wasman.2020.05.048.

[7] Steyn, Z. C., Babafemi, A. J., Fataar, H., & Combrinck, R. (2021). Concrete containing waste recycled glass, plastic and rubber as sand replacement. Construction and Building Materials, 269, 121242. doi:10.1016/j.conbuildmat.2020.121242.

[8] Jain, A., Siddique, S., Gupta, T., Jain, S., Sharma, R. K., & Chaudhary, S. (2021). Evaluation of concrete containing waste plastic shredded fibers: Ductility properties. Structural Concrete, 22(1), 566–575. doi:10.1002/suco.201900512.

[9] Anandan, S., & Alsubih, M. (2021). Mechanical strength characterization of plastic fiber reinforced cement concrete composites. Applied Sciences (Switzerland), 11(2), 1–21. doi:10.3390/app11020852.

[10] Khalid, F. S., Irwan, J. M., Ibrahim, M. H. W., Othman, N., & Shahidan, S. (2018). Performance of plastic wastes in fiber-reinforced concrete beams. Construction and Building Materials, 183, 451–464. doi:10.1016/j.conbuildmat.2018.06.122.

[11] Nistratov, A. V., Klimenko, N. N., Pustynnikov, I. V., & Vu, L. K. (2022). Thermal Regeneration and Reuse of Carbon and Glass Fibers from Waste Composites. Emerging Science Journal, 6(5), 967-984. doi:10.28991/ESJ-2022-06-05-04.

[12] Záleská, M., Pavlíková, M., Pokorný, J., Jankovský, O., Pavlík, Z., & Černý, R. (2018). Structural, mechanical and hygrothermal properties of lightweight concrete based on the application of waste plastics. Construction and Building Materials, 180, 1–11. doi:10.1016/j.conbuildmat.2018.05.250.

[13] Ruiz-Herrero, J. L., Velasco Nieto, D., López-Gil, A., Arranz, A., Fernández, A., Lorenzana, A., Merino, S., De Saja, J. A., & Rodríguez-Pérez, M. Á. (2016). Mechanical and thermal performance of concrete and mortar cellular materials containing plastic waste. Construction and Building Materials, 104, 298–310. doi:10.1016/j.conbuildmat.2015.12.005.

[14] Farajzadehha, S., Ziaei Moayed, R., & Mahdikhani, M. (2020). Comparative study on uniaxial and triaxial strength of plastic concrete containing nano silica. Construction and Building Materials, 244, 118212. doi:10.1016/j.conbuildmat.2020.118212.

[15] Ahmad, F., Qureshi, M. I., & Ahmad, Z. (2022). Influence of nano graphite platelets on the behavior of concrete with E-waste plastic coarse aggregates. Construction and Building Materials, 316, 125980. doi:10.1016/j.conbuildmat.2021.125980.

[16] Punitha, V., Sakthieswaran, N., & Babu, O. G. (2020). Experimental investigation of concrete incorporating HDPE plastic waste and metakaolin. Materials Today: Proceedings, 37(Part 2), 1032–1035. doi:10.1016/j.matpr.2020.06.288.

[17] Balasubramanian, B., Gopala Krishna, G. V. T., Saraswathy, V., & Srinivasan, K. (2021). Experimental investigation on concrete partially replaced with waste glass powder and waste E-plastic. Construction and Building Materials, 278, 122400. doi:10.1016/j.conbuildmat.2021.122400.

[18] Liu, T., Nafees, A., khan, S., Javed, M. F., Aslam, F., Alabduljabbar, H., Xiong, J. J., Ijaz Khan, M., & Malik, M. Y. (2022). Comparative study of mechanical properties between irradiated and regular plastic waste as a replacement of cement and fine aggregate for manufacturing of green concrete. Ain Shams Engineering Journal, 13(2), 101563. doi:10.1016/j.asej.2021.08.006.

[19] Khan, M. I., Sutanto, M. H., Napiah, M. Bin, Khan, K., & Rafiq, W. (2021). Design optimization and statistical modeling of cementitious grout containing irradiated plastic waste and silica fume using response surface methodology. Construction and Building Materials, 271, 121504. doi:10.1016/j.conbuildmat.2020.121504.

[20] Çolak, A. B., Akçaözoğlu, K., Akçaözoğlu, S., & Beller, G. (2021). Artificial Intelligence Approach in Predicting the Effect of Elevated Temperature on the Mechanical Properties of PET Aggregate Mortars: An Experimental Study. Arabian Journal for Science and Engineering, 46(5), 4867–4881. doi:10.1007/s13369-020-05280-1.

[21] Çelik, F., Çolak, A. B., Yıldız, O., & Bozkır, S. M. (2022). An Experimental Investigation on Workability and Bleeding Features. ACI Materials Journal, 119(5), 63–76. doi:10.14359/51735949.

[22] Çolak, A. B., Yıldız, O., Çelik, F., & Bozkır, S. M. (2022). Developing Prediction Model on Workability Parameters of Ultrasonicated Nano Silica (n-SiO2) and Fly Ash Added Cement-Based Grouts by Using Artificial Neural Networks. Advances in Civil Engineering Materials, 11(1), 20210124. doi:10.1520/acem20210124.

[23] Rezvan, S., Moradi, M. J., Dabiri, H., Daneshvar, K., Karakouzian, M., & Farhangi, V. (2023). Application of Machine Learning to Predict the Mechanical Characteristics of Concrete Containing Recycled Plastic-Based Materials. Applied Sciences (Switzerland), 13(4), 2033. doi:10.3390/app13042033.

[24] Sau, D., Hazra, T., & Shiuly, A. (2023). Assessment of Sustainable Green Concrete Properties Using Recycled Plastic Waste as Replacement for Fine Aggregate Using Machine Learning Technique. Composites: Mechanics, Computations, Applications, 14(2), 1–12. doi:10.1615/COMPMECHCOMPUTAPPLINTJ.2022044775.

[25] Ofuyatan, O. M., Agbawhe, O. B., Omole, D. O., Igwegbe, C. A., & Ighalo, J. O. (2022). RSM and ANN modelling of the mechanical properties of self-compacting concrete with silica fume and plastic waste as partial constituent replacement. Cleaner Materials, 4, 100065. doi:10.1016/j.clema.2022.100065.

[26] Nafees, A., Khan, S., Javed, M. F., Alrowais, R., Mohamed, A. M., Mohamed, A., & Vatin, N. I. (2022). Forecasting the Mechanical Properties of Plastic Concrete Employing Experimental Data Using Machine Learning Algorithms: DT, MLPNN, SVM, and RF. Polymers, 14(8), 1583. doi:10.3390/polym14081583.

[27] Jamii, J., Mansouri, M., Trabelsi, M., Mimouni, M. F., & Shatanawi, W. (2022). Effective artificial neural network-based wind power generation and load demand forecasting for optimum energy management. Frontiers in Energy Research, 10. doi:10.3389/fenrg.2022.898413.

[28] Rehman, K. U., Çolak, A. B., & Shatanawi, W. (2022). Artificial Neural Networking (ANN) Model for Convective Heat Transfer in Thermally Magnetized Multiple Flow Regimes with Temperature Stratification Effects. Mathematics, 10(14), 2394. doi:10.3390/math10142394.

[29] Rehman, K. U., Shatanawi, W., & Çolak, A. B. (2023). Artificial neural networking estimation of skin friction coefficient at cylindrical surface: a Casson flow field. European Physical Journal Plus, 138(1), 1–15. doi:10.1140/epjp/s13360-023-03704-z.

[30] Quadros, J. D., Nagpal, C., Khan, S. A., Aabid, A., & Baig, M. (2022). Investigation of suddenly expanded flows at subsonic Mach numbers using an artificial neural networks approach. PLOS ONE, 17(10), e0276074. doi:10.1371/journal.pone.0276074.

[31] Moriyama, M., Takeuchi, M., Uwate, Y., & Nishio, Y. (2016). Firefly Algorithm combined with chaotic map. IEEE Workshop on Nonlinear Circuit Networks, 9-10 December, 2016, Tokushima, Japan.

[32] Umar, I. K., Gökçekuş, H., & Nourani, V. (2022). An intelligent soft computing technique for prediction of vehicular traffic noise. Arabian Journal of Geosciences, 15(19), 1571. doi:10.1007/s12517-022-10858-0.

[33] Muthukumar, M., Mohan, D., & Rajendran, M. (2003). Optimization of mix proportions of mineral aggregates using Box Behnken design of experiments. Cement and Concrete Composites, 25(7), 751–758. doi:10.1016/S0958-9465(02)00116-6.

[34] Wang, W. C., Xu, D. M., Chau, K. W., & Chen, S. (2013). Improved annual rainfall-runoff forecasting using PSO-SVM model based on EEMD. Journal of Hydroinformatics, 15(4), 1377–1390. doi:10.2166/hydro.2013.134.

[35] Yasar, A., Bilgili, M., & Simsek, E. (2012). Water Demand Forecasting Based on Stepwise Multiple Nonlinear Regression Analysis. Arabian Journal for Science and Engineering, 37(8), 2333–2341. doi:10.1007/s13369-012-0309-z.

[36] Adamu, M., Çolak, A. B., Ibrahim, Y. E., Haruna, S. I., & Hamza, M. F. (2023). Prediction of Mechanical Properties of Rubberized Concrete Incorporating Fly Ash and Nano Silica by Artificial Neural Network Technique. Axioms, 12(1), 81. doi:10.3390/axioms12010081.

[37] Adamu, M., Haruna, S. I., Malami, S. I., Ibrahim, M. N., Abba, S. I., & Ibrahim, Y. E. (2022). Prediction of compressive strength of concrete incorporated with jujube seed as partial replacement of coarse aggregate: a feasibility of Hammerstein–Wiener model versus support vector machine. Modeling Earth Systems and Environment, 8(3), 3435–3445. doi:10.1007/s40808-021-01301-6.

[38] Taylor, K. E. (2001). Summarizing multiple aspects of model performance in a single diagram. Journal of Geophysical Research Atmospheres, 106(D7), 7183–7192. doi:10.1029/2000JD900719.

[39] Yaseen, Z. M., Deo, R. C., Hilal, A., Abd, A. M., Bueno, L. C., Salcedo-Sanz, S., & Nehdi, M. L. (2018). Predicting compressive strength of lightweight foamed concrete using extreme learning machine model. Advances in Engineering Software, 115, 112–125. doi:10.1016/j.advengsoft.2017.09.004.

[40] Zhu, S., & Heddam, S. (2020). Prediction of dissolved oxygen in urban rivers at the three Gorges reservoir, China: Extreme learning machines (ELM) versus artificial neural network (ANN). Water Quality Research Journal, 55(1), 106–118. doi:10.2166/WQRJ.2019.053.

[41] Haruna, S. I., Malami, S. I., Adamu, M., Usman, A. G., Farouk, A., Ali, S. I. A., & Abba, S. I. (2021). Compressive Strength of Self-Compacting Concrete Modified with Rice Husk Ash and Calcium Carbide Waste Modeling: A Feasibility of Emerging Emotional Intelligent Model (EANN) Versus Traditional FFNN. Arabian Journal for Science and Engineering, 46(11), 11207–11222. doi:10.1007/s13369-021-05715-3.